NANO REVIEWS

COACTION PUBLISHING

SHORT COMMUNICATION

Ordered arrays of multiferroic epitaxial nanostructures

Ionela Vrejoiu*, Alessio Morelli, Daniel Biggemann and Eckhard Pippel

Max Planck Institute of Microstructure Physics, Halle, Germany

Received: 10 June 2011; Revised: 5 August 2011; Accepted: 7 August 2011; Published: 4 October 2011

Abstract

Epitaxial heterostructures combining ferroelectric (FE) and ferromagnetic (FiM) oxides are a possible route to explore coupling mechanisms between the two independent order parameters, polarization and magnetization of the component phases. We report on the fabrication and properties of arrays of hybrid epitaxial nanostructures of FiM $NiFe_2O_4$ (NFO) and FE $PbZr_{0.52}Ti_{0.48}O_3$ or $PbZr_{0.2}Ti_{0.8}O_3$, with large range order and lateral dimensions from 200 nm to 1 micron.

Methods: The structures were fabricated by pulsed-laser deposition. High resolution transmission electron microscopy and high angle annular dark-field scanning transmission electron microscopy were employed to investigate the microstructure and the epitaxial growth of the structures. Room temperature ferroelectric and ferrimagnetic domains of the heterostructures were imaged by piezoresponse force microscopy (PFM) and magnetic force microscopy (MFM), respectively.

Results: PFM and MFM investigations proved that the hybrid epitaxial nanostructures show ferroelectric and magnetic order at room temperature. Dielectric effects occurring after repeated switching of the polarization in large planar capacitors, comprising ferrimagnetic $NiFe_2O_4$ dots embedded in ferroelectric $PbZr_{0.52}Ti_{0.48}O_3$ matrix, were studied.

Conclusion: These hybrid multiferroic structures with clean and well defined epitaxial interfaces hold promise for reliable investigations of magnetoelectric coupling between the ferrimagnetic / magnetostrictive and ferroelectric / piezoelectric phases.

Keywords: *multiferroic composites*; *epitaxial nanostructures*; *pulsed-laser deposition*; *piezoresponse force microscopy*; *magnetic force microscopy*

Epitaxial multiferroic heterostructures combining phases of ferroelectric (FE) and ferromagnetic or ferrimagnetic (FiM) materials are a viable alternative to artificially create magnetoelectric (ME) materials with strong coupling between the polarization and magnetization at room temperature (RT). The ME composites have a number of advantages over the intrinsic single phase ME materials, the later showing usually much weaker ME effects and often only at low temperatures (1). In composites, the ME coupling arises chiefly from extrinsic mechanisms, for example, as a product tensor property, in which the FiM phase is magnetostrictive and FE phase is piezoelectric and the coupling occurs via elastic interaction (2–5). Various geometries with different connectivity schemes have been proposed for bulk ME composites (2). For thin film composites fabricated on single crystal substrates, few issues are of high concern when designing the best combination to achieve large ME effects: (1) the physical properties of the individual phases (ordering temperatures, magnetostriction and piezoelectric coefficients, anisotropy constants, magnitude of magnetization, and polarization), (2) the structural compatibility of the two materials for heteroepitaxial growth and the quality of the interfaces with the substrate and between FE and magnetic phases, and (3) the choice of suitable geometrical arrangements of the two phases for diminishing the effects of clamping to the bulk substrate. The first two issues lead us to select as suitable candidates FE perovskite oxides (e.g. $PbZr_xTi_{1-x}O_3$ [PZT]) and

insulating FiM spinel oxides (e.g. $NiFe_2O_4$ [NFO]) or $CoFe_2O_4$. To circumvent the clamping to the bulk substrate, which greatly inhibits the elastic interaction between the FE and FiM phases, the fabrication of nanostructured epitaxial ME composite films is desirable. Thus, the high-quality epitaxial interfaces can be still preserved, but the magnetostrictive and piezoelectric phases are much less laterally clamped to the bulk substrate. Epitaxial ME composite nanostructures have been fabricated by various *in situ* techniques. One method is a self-assembly process in which the FE phase (e.g. $BaTiO_3$, $PbTiO_3$, or $BiFeO_3$) and FiM phase ($CoFe_2O_4$) separate, resulting in FiM nanopillars embedded in a FE matrix, the pillars having a hexagonal arrangement (6–9). The drawback is that the nanostructures form with rather irregular shape and with poor ordering over extended areas. Other approach is to employ stencil masks during the fabrication, such as porous anodic aluminum oxide (AAO) ultrathin membranes attached to the substrate, to produce mesoscopically ordered arrays of epitaxial nanostructures of sizes well below 100 nm, as demonstrated in (10, 11).

We report on the fabrication and properties of large scale-ordered heteroepitaxial structures of FiM NFO and FE $PbZr_{0.52}Ti_{0.48}O_3$ (PZT52/48) or $PbZr_{0.2}Ti_{0.8}O_3$ (PZT20/80), with lateral dimensions from about 200 nm to 1 μm. Among the PZT solid solution compositions, PZT52/48 has the largest piezoelectric coefficients and polarization of ≈ 50 $\mu C/cm^2$, whereas for PZT20/80 epitaxial films we reported record values of polarization of ≈ 100 $\mu C/cm^2$ (12). The dot structures were fabricated by pulsed-laser deposition (PLD) (13). We employed stencil masks consisting of amorphous silicon nitride (SiN) membranes (few 100 nm thick) produced on silicon (Si) wafers, with ordered circular apertures (200–800 nm diameter). The stencils can be attached mechanically to single crystal substrates of Nb-doped $SrTiO_3$(100) or $SrRuO_3$-coated $SrTiO_3$(100). During the growth of the dots, the substrates were heated at temperatures of 550–600°C. Such stencil masks have been used to produce Bi_2FeCrO_6, $BaTiO_3$, and PZT nanostructures by PLD (14–16). The advantage of this kind of masks over the AAO masks is that the order of the nanoapertures is almost perfect over entire area, with very low density of defects, whereas the domains of hexagonally ordered pores of AAO membranes extend only over several microns areas. Moreover, the AAO masks are very difficult to be completely removed mechanically from the substrate after the epitaxial nanostructures have been grown at elevated temperatures. Large pieces of membrane remain stuck on the substrate. Chemical postwet etching of the AAO masks can be done, which, in turn, can damage the fabricated structures. These issues of the AAO-made nanostructures hinder reliable and quantitative studies by electrical measurements, since such measurements have to be performed either through large top metallic electrodes deposited on top of areas containing many structures or locally, on individual structures, by scanning probe microscopy methods, such as piezoresponse force microscopy (PFM) and magnetic force microscopy (MFM). One should avoid *quick and dirty* fabrication methods to produce nanostructures intended for subtle fundamental physical investigations, like the manifestation of coupling between the polarization and the magnetization of the two phases. The effects of the coupling may be monitored by imaging the FE and/or the FiM domain changes upon switching one of the order parameters, as has been shown by Zavaliche et al. (17). Moreover, designing stencil masks so that multiferroic heterostructures with particular topologies are achieved may allow for the optimization of the ME effects (18).

The microstructure of the nanostructures was studied by transmission electron microscopy (TEM) in a CM20T Philips microscope and by high angle annular dark-field scanning TEM (HAADF-STEM), with a Titan 80–300 FEI microscope. We investigated the room temperature FE and FiM domain structures by PFM and MFM, respectively, using a commercial atomic force microscope (MFP-3D Asylum Research). The effects of the switching of the FE polarization on the magnetic domains of the FiM nanostructures are to be studied.

Fig. 1 shows atomic force microscopy (tapping mode) height-images of perfectly ordered epitaxial circular NFO dots made through a stencil with 200 nm diameter pores (Fig. 1a) and of larger NFO dots (stencil with 800 nm diameter apertures) embedded in a PZT52/48 film (Fig. 1b).

Superconducting quantum interference device (SQUID) magnetometry measurements (not shown here) indicated that NFO dots (stencil with 800-nm-diameter apertures) grown on an Nb:STO(100) substrate are ordered ferromagnetically at 300 K and have the magnetic easy axis in the out-of-plane direction. MFM measurements at RT enabled us to image the magnetic domains of these NFO dots (Fig. 2a) and also of NFO dots (stencil with 400 nm diameter apertures) embedded in a 20-nm-thin PZT20/80 film, all epitaxially grown on a $SrRuO_3/SrTiO_3$(100) substrate (Fig. 2b). Though probed through a 20-nm-thin nonmagnetic PZT layer, the FiM domain contrast of the NFO dots is quite well visible in Fig. 2b. In between the NFO dots, the PZT20/80 film has a polarization pointing upward, resulting in bright contrast in the PFM image (Fig. 2c). A stable domain of opposite orientation of the polarization (uniform dark contrast, with at least 44-h retention) could be written in the FE film by applying a suitably large bias voltage during scanning that area in the PFM mode (Fig. 2c). The piezoresponse phase hysteresis loop measured on top of a PZT20/80/NFO dot is shown in Fig. 2d and it indicates good switching properties of the NFO/PZT

Citation: Nano Reviews 2011, **2**: 7364 - DOI: 10.3402/nano.v2i0.7364

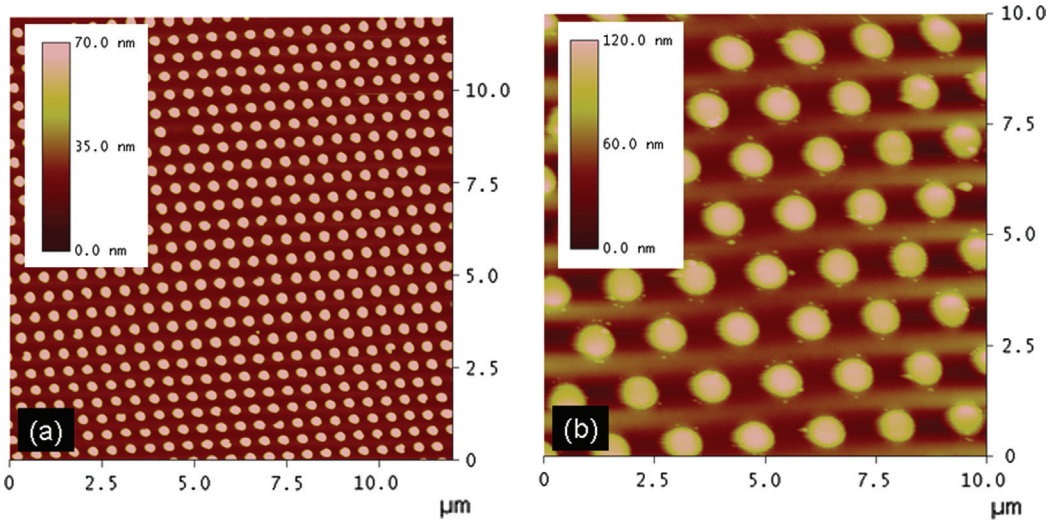

Fig. 1. Atomic force microscopy height-images of arrays of ordered epitaxial (a) $NiFe_2O_4$ dots made through a stencil mask with 200 nm diameter pores (12 × 12 μm large area) and of (b) $NiFe_2O_4$ dots made with a stencil with 800 nm diameter pores and embedded in an epitaxial $PbZr_{0.52}Ti_{0.48}O_3$ film (10 μm × 10 μm large area).

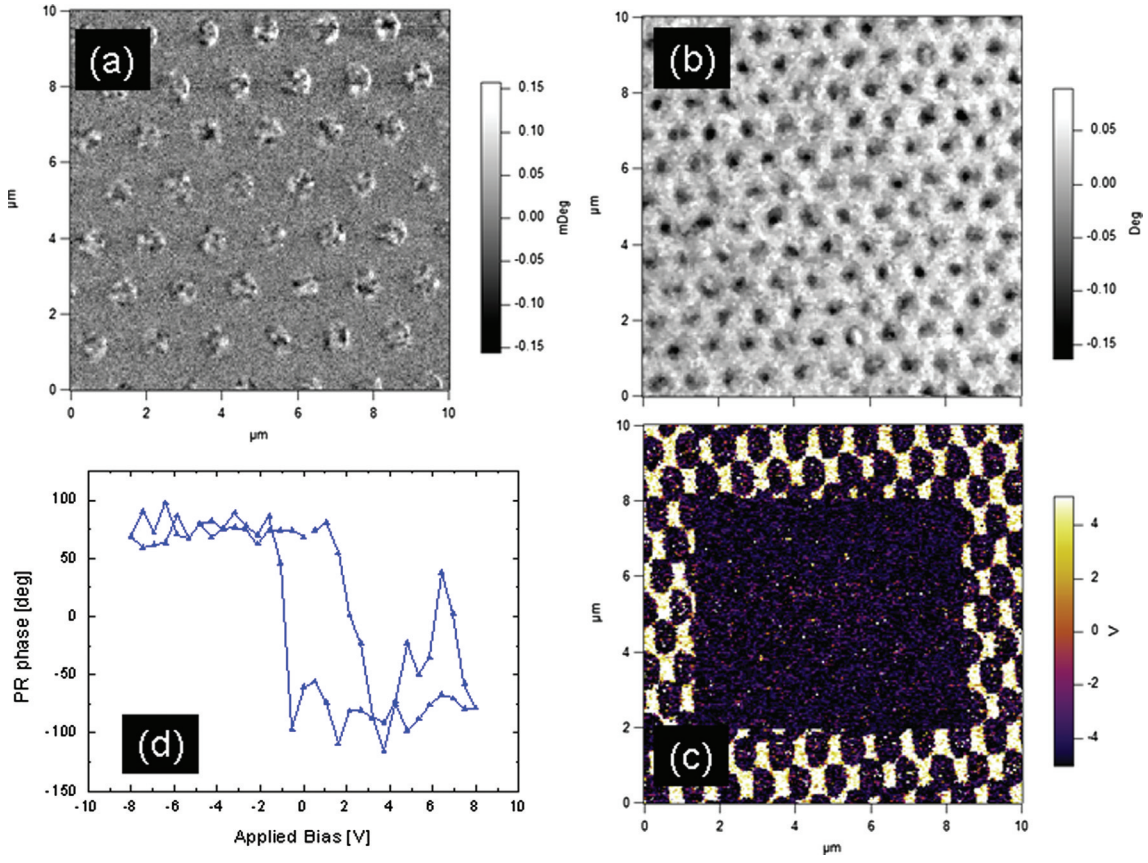

Fig. 2. Magnetic force microscopy phase image of (a) $NiFe_2O_4$ dots (stencil with 800 nm pores) and of (b) $NiFe_2O_4$ dots (stencil with 400 nm pores) embedded in a ferroelectric 20 nm thick PZT20/80 film. In (c) a piezoresponse force microscopy phase image of the same sample as in (b) is shown, in which the polarization of the PZT20/80 film in central area was switched (uniform dark contrast) by applying a suitable dc voltage during scanning. The piezoresponse phase hysteresis loop measured on top of a PZT20/80/$NiFe_2O_4$ dot is shown in (d). All images are 10 μm × 10 μm large.

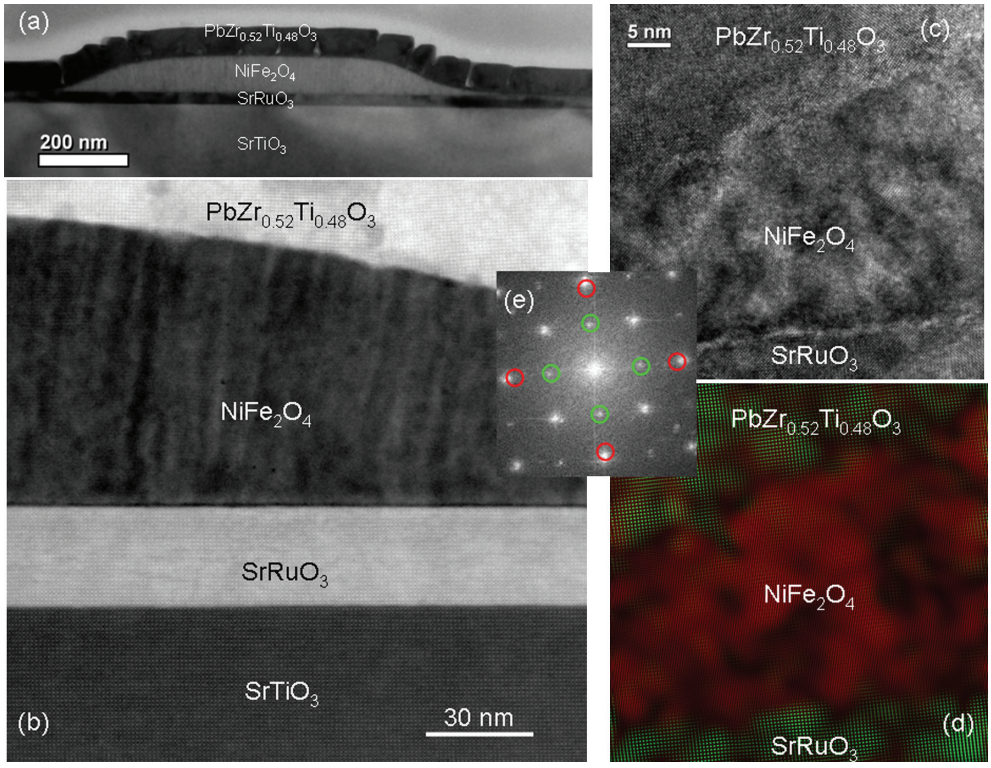

Fig. 3. (a) Cross-section TEM and (b) Z-contrast STEM micrographs of an epitaxial $NiFe_2O_4$ dot embedded in a $PbZr_{0.52}Ti_{0.48}O_3$ film grown on a $SrRuO_3$-coated $SrTiO_3$ (100) substrate. (c) High resolution TEM image taken close to an edge of a $NiFe_2O_4$ dot and (d) the corresponding dark-field reconstructed image, using the selected reflections of the spinel (red) and perovskite (green) structures, as marked in the fast Fourier transform pattern shown in (e).

heterostructures. These preliminary studies show that the NFO/PZT heterostructures have good FiM and FE properties at RT.

The microstructure and the chemical details of the NFO dots embedded in a PZT52/48 film, imaged by atomic force microscopy (AFM) in Fig. 1b, were

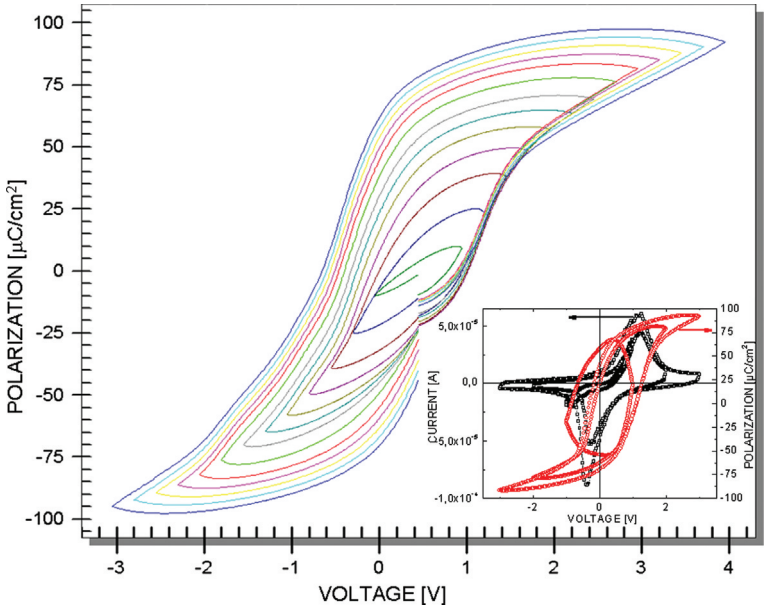

Fig. 4. Polarization hysteresis loops measured on top of $NiFe_2O_4$ dots (stencil with 400 nm diameter pores), embedded in a PZT52/48 film. The inset shows the polarization loops measured on the bare PZT52/48 film, away from the area with $NiFe_2O_4$ dots.

Citation: Nano Reviews 2011, **2**: 7364 - DOI: 10.3402/nano.v2i0.7364

investigated by TEM and Z-contrast STEM. Fig. 3a shows a low-magnification cross-section TEM micrograph of one NFO structure and the epitaxial layer of PZT52/48 grown on top. Fig. 3b is a Z-contrast STEM micrograph of the same structure, allowing a closer look at the microstructure and the interface between the NFO dot and the embedding PZT52/48 epitaxial film, and also to analyze the composition. In Z-contrast STEM micrographs, the intensity is proportional to the atomic number Z of the constituent elements. Electron energy loss spectra allowed us to quantify the ratio between the Ni and Fe content of the NFO dots, and Ni/Fe = 0.51 ± 0.072 ratio was obtained, indicating that the dots have the stoichiometry required by the spinel structure. Moreover, analysis of an HRTEM micrograph (Fig. 3c), showing part of the $SrRuO_3$ (SRO) bottom electrode of the NFO dot and of the embedding PZT52/48 film, proved that the entire heterostructure is epitaxial. The Fourier filtering using the selected spots as shown in the fast Fourier transform pattern (Fig. 3e) allowed us to make dark-field reconstruction of the HRTEM image (Fig. 3d). The reconstructed image proves that the NFO dot has the expected spinel structure, with almost twice as large lattice parameters than the cubic STO substrate, while the SRO and PZT52/48 layers have perovskite pseudocubic structures (11, 19).

Platinum top contacts were deposited by sputtering (60 × 60 μm squares) both on top of the areas where the embedded NFO dots are and on the bare PZT52/48 film, in order to measure the switchable FE polarization. The hysteresis loops measured at RT and 1 kHz on a Pt electrode on an area with PZT52/48/NFO dots (stencil with 400-nm-diameter pores) is shown in Fig. 4. The inset of Fig. 4 shows the polarization loops measured on the Pt electrodes sputtered on bare PZT52/48 film of the same sample, away from the area with NFO structures. The values of the remnant polarizations for the two types of pristine capacitors are very similar. However, the main difference consists in the opposite direction of the imprint of the loops, indicating the existence of internal electric fields of opposite directions in the two types of capacitors. This points out that the direction and magnitude of imprint are most probably related to chemically different interfaces, with different density of defects. The same behavior of the hysteresis imprint was observed also for a sample in which the NFO dots were grown through a stencil with 800-nm-diameter pores and then embedded in a PZT52/48 film, fabricated under the same conditions. Fig. 5 summarizes polarization and capacitance measurements performed on an electrode on top of the area with PZT52/48/NFO dots (800 nm diameter). Fig. 5a shows the pristine behavior of the polarization loop, whereas Fig. 5b shows the loop measured after a polarization

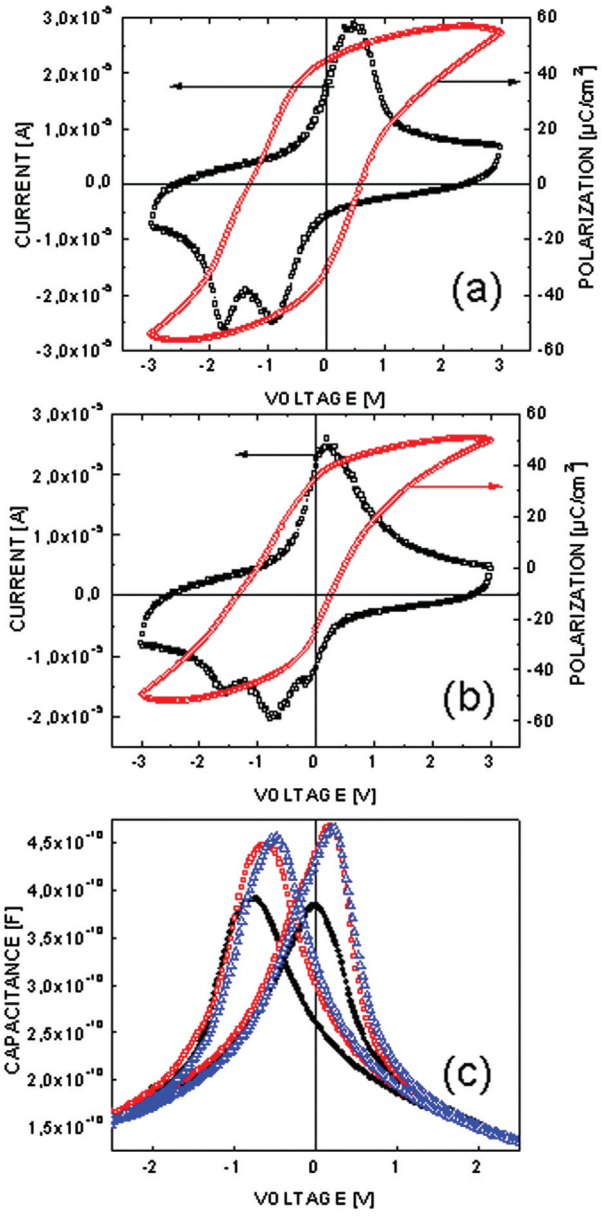

Fig. 5. Polarization hysteresis loops measured at 1 kHz and RT through Pt electrodes on top of $NiFe_2O_4$ dots (stencil with 800 nm diameter pores) embedded in a PZT52/48 film: (a) on the pristine capacitor and (b) of the same capacitor after a fatigue experiment. (c) Capacitance versus bias voltage measurements performed before (black solid circles) and after two consecutive polarization fatigue experiments (red open squares and blue open triangles).

fatigue experiment was performed (for 10^6 cycles at 1 kHz) on the same capacitor. The switched polarization of the capacitor did not undergo major changes, except for slight changes in the switching current peaks profile for negative polarity and an even further imprint of the loop toward negative voltage. However, a more obvious change occurred after the first fatigue process for the

capacitance of the contact. Small signal capacitance versus bias voltage butterfly loops (at 1 kHz and RT), before (on the pristine contact) and after two consecutive polarization fatigue experiments, are shown in Fig. 5c. A significant increase of the maximum and zero bias capacitance occurred after the first fatigue and much less change of the butterfly loop took place after the second fatigue, indicating a stabilization of the capacitance behavior. This behavior results most likely from the fact that during the first fatigue experiment trapping/detrapping of charge carriers occurred possibly at the inner interfaces of the NFO dots and the FE PZT52/48 embedding film, and at the interfaces with the electrodes. In addition, movement of FE domain walls toward stable configurations may have taken place. These observations are important for further magneto-dielectric measurements, when the behavior of the capacitance of the multiferroic composite structures will be studied under applied magnetic field (11). As already pointed out by Catalan (20), often the existence of a magnetocapacitance effect is mistaken as a proof of multiferroic behavior in a new material system; however, magnetocapacitance effects may occur without any ME coupling. Our measurements show that, additionally, one has to pay attention first to the state of the capacitor and keep record of the measurements performed on it, because an increase or variation of the capacitance can arise even without application of an external magnetic field. Our measurements recommend that repeated polarization switching of the multiferroic capacitors (until a stable value of the capacitance is achieved) should be performed prior to magnetocapacitance measurements.

In summary, we fabricated large arrays of ordered all-epitaxial hybrid FiM/FE structures, consisting of dots of NFO and thin films of $PbZr_{0.52}Ti_{0.48}O_3$ (PZT52/48) or $PbZr_{0.2}Ti_{0.8}O_3$ (PZT20/80). The dots were proven to have FiM order at RT, by means of SQUID magnetometry and MFM. The FE properties of the structures were probed by PFM and by macroscopic measurements through platinum top electrodes. These hybrid multiferroic structures with clean and well-defined epitaxial interfaces hold promise for reliable investigations of ME coupling between the FiM/magnetostrictive and FE/piezoelectric phases. Further studies by means of X-ray photoemission electron microscopy are planned to investigate possible changes of the magnetic structure of the FiM dots upon switching the polarization in the FE film.

Conflict of interest and funding

There is no conflict of interest in the present study for any of the authors.

Acknowledgements

We are grateful to Norbert Schammelt for the FIB preparation of the TEM specimens and to Dr. Michael Ziese (University of Leipzig) for SQUID magnetometry of the ferrite dots.

References

1. Vaz CAF, Hoffman J, Ahn CH, Ramesh R. Magnetoelectric coupling effect in multiferroic complex oxide composite structures. Adv Mater 2010; 22: 2900–18.
2. Nan C-W, Bichurin ME, Dong S, Viehland D, Srinivasan G. Multiferroic magnetoelectric composites: hystorical perspective, status, and future directions. J Appl Phys 2008; 103: 031101–23.
3. Srinivasan G. Magnetoelectric composites. Annu Rev Mater Res 2010; 40: 153–16.
4. Ma J, Hu J, Li Z, Nan C-W. Recent progress in multiferroic magnetoelectric composites: from bulk to thin films. Adv Mater 2011; 23: 1062–16.
5. Kukhar VG, Pertsev NA, Kholkin AL. Thermodynamic theory of strain-mediated direct magnetoelectric effect in multiferroic film-substrate hybrids. Nanotechnol 2010; 21: 265701–11.
6. Zheng H, Wang J, Lofland SE, Ma Z, Mohaddes-Ardabili L, Zhao T, et al. Multiferroic $BaTiO_3$-$CoFe_2O_4$ Nanostructures. Science 2004; 303: 661–3.
7. Slutsker J, Levin I, Li J, Artemev A, Roytburd AL. Effect of elastic interactions on the self-assembly of multiferroic nanostructures in epitaxial films. Phys Rev B 2006; 73: 184127–4.
8. Yan L, Yang Y, Wang Z, Xing Z, Li J, Viehland D. Review of magnetoelectric perovskite-spinel self-assembled nano-composite thin films. J Mater Sci 2009; 44: 5080–15.
9. Dix N, Muralidharan R, Rebled J-M, Estradé S, Peiró F, Varela M, et al. Selectable spontaneous polarization direction and magnetic anisotropy in $BiFeO_3$-$CoFe_2O_4$ epitaxial nanostructures. ACS Nano 2010; 4: 4955–7.
10. Lee W, Han H, Lotnyk A, Schubert AM, Senz S, Alexe M, et al. Individually addressable epitaxial ferroelectric nanocapacitor arrays with near Tb inch^{-2} density. Nat Nanotechnol 2008; 3: 402–6.
11. Gao XS, Rodriguez BJ, Liu L, Birajdar B, Pantel D, Ziese M, et al. Microstructure and properties of well-ordered multiferroic $Pb(Zr,Ti)O_3$/$CoFe_2O_4$ nanocomposites. ACS Nano 2010; 4: 1099–1107.
12. Vrejoiu I, Le Rhun G, Pintilie L, Hesse D, Alexe M, Gösele U. Intrinsic ferroelectric properties of strained tetragonal $PbZr_{0.2}Ti_{0.8}O_3$ obtained on layer-by-layer grown, defect-free single-crystalline films. Adv Mater 2006; 18: 1657–61.
13. Baeurle D. Laser processing and chemistry, third ed. Berlin: Springer; 2000.
14. Nechache R, Cojocaru VC, Harnagea C, Nauenheim C, Niklaus M, Ruediger A, et al. Epitaxial patterning of Bi_2FeCrO_6 double perovskite nanostructures: multiferroic at room temperature. Adv Mater 2011; 23: 1724–6.
15. Cojocaru CV, Nechache R, Harnagea C, Pignolet A, Rosei F. Nanoscale patterning of functional perovskite-type complex oxides by pulsed laser deposition through a nanostencil. Appl Surf Sci 2010; 256: 4777–83.
16. te Riele PM, Rijnders G, Blank DHA. Ferroelectric devices created by pressure modulated stencil deposition. Appl Phys Lett 2008; 93: 233109–3.
17. Zavaliche F, Zhao T, Zheng H, Straub F, Cruz MP, Yang P-L, et al. Electrically assisted magnetic recording in multiferroic nanostructures. Nano Lett 2007; 7: 1586–90.

Citation: Nano Reviews 2011, **2**: 7364 - DOI: 10.3402/nano.v2i0.7364

18. Sun KH, Kim YY. Design of magnetoelectric multiferroic heterostructures by topology optimization. J Phys D Appl Phys 2011; 44: 185003–8.
19. Gao XS, Bao DH, Birajdar B, Habisreuther T, Mattheis R, Schubert MA, et al. Switching magnetic anisotropy in epitaxial $CoFe_2O_4$ thin films induced by $SrRuO_3$ buffer layer. J Phys D Appl Phys 2009; 42: 175006–9.
20. Catalan G. Magnetocapacitance without magnetoelectric coupling. Appl Phys Lett 2006; 88: 102902–3.

***Ionela Vrejoiu**
Max Planck institute of Microstructure Physics
Weinberg 2
DE-06120 Halle
Germany
Email: vrejoiu@mpi-halle.de